NeuroImage: Clinical 13 (2017) 446–454

Contents lists available at ScienceDirect

NeuroImage: Clinical

journal homepage: www.elsevier.com/locate/ynicl

Brain correlates of spike and wave discharges in GLUT1 deficiency syndrome

Anna Elisabetta Vaudano[a,b,1], Sara Olivotto[c,1], Andrea Ruggieri[a], Giuliana Gessaroli[b], Valentina De Giorgis[c], Antonia Parmeggiani[d,e], Pierangelo Veggiotti[c,f,*], Stefano Meletti[a,b]

[a] Department of Biomedical, Metabolic, and Neural Sciences, University of Modena and Reggio Emilia, Modena, Italy
[b] N.O.C.S.A.E. Hospital, AUSL Modena, 41100 Modena, Italy
[c] Brain and Behavior Department, University of Pavia, Pavia, Italy
[d] Child Neurology and Psychiatry Unit, Policlinico S. Orsola-Malpighi, Bologna, Italy
[e] Department of Medical and Surgical Sciences, University of Bologna, Italy
[f] Department of Child Neurology and Psychiatry, "C. Mondino" National Neurological Institute, Pavia, Italy

ARTICLE INFO

Article history:
Received 13 July 2016
Received in revised form 4 November 2016
Accepted 19 December 2016
Available online 21 December 2016

Keywords:
GLUT1
Generalized spike-and-wave discharges
Basal ganglia
Genetic generalized epilepsy
Absence seizure

ABSTRACT

Purpose: To provide imaging biomarkers of generalized spike-and-wave discharges (GSWD) in patients with GLUT1 deficiency syndrome (GLUT1DS).
Methods: Eighteen GLUT1DS patients with pathogenetic mutation in SLC2A1 gene were studied by means of Video-EEG simultaneously recorded with functional MRI (VideoEEG-fMRI). A control group of sex and age-matched patients affected by Genetic Generalized Epilepsy (GGE) with GSWD were investigated with the same protocol. Within and between groups comparison was performed as appropriated. For GLUT1DS, correlations analyses between the contrast of interest and the main clinical measurements were provided.
Results: EEG during fMRI revealed interictal GSWD in 10 GLUT1DS patients. Group-level analysis showed BOLD signal increases at the premotor cortex and putamen. With respect to GGE, GLUT1DS patients demonstrated increased neuronal activity in the putamen, precuneus, cingulate cortex, SMA and paracentral lobule. Whole-brain correlation analyses disclosed a linear relationship between the GSWD-related BOLD changes and the levels of glycorrhachia at diagnosis over the sensory-motor cortex and superior parietal lobuli.
Conclusion: The BOLD dynamics related to GSWD in GLUT1DS are substantially different from typical GGE showing the former an increased activity in the premotor-striatal network and a decrease in the thalamus. The revealed hemodynamic maps might represent imaging biomarkers of GLUT1DS, being potentially useful for a precocious diagnosis of this genetic disorder.

1. Introduction

Glucose transporter type I deficiency syndrome (GLUT1DS) is a treatable encephalopathy, caused by a defect of glucose uptake, mediated by GLUT1, at the blood brain barrier and into brain cells due to mutations in *SLC2A1* gene (solute carrier family 2 member 1) (Wang et al., 2005). The classical phenotype includes a range of complex movement disorders, drug-resistance epilepsy, mental retardation, and acquired microcephaly (De Vivo et al., 1991; Seidner et al., 1998). Less severe disorders mainly characterized by paroxysmal exercised-induced dyskinesia (PED) and 'generalized epilepsies', either alone or in combination, have been reported (Arsov et al., 2012a; Striano et al., 2012; Suls et al., 2008, 2009). When epilepsy is the main symptom, absence seizures (AS), mainly with early onset, seem to be the most frequent clinical expression of *SLC2A1* mutations and in individual cases AS may be phenotypically indistinguishable from absences of the genetic generalized epilepsies (GGE; formerly known as idiopathic generalized epilepsies) (Arsov et al., 2012a; Mullen et al., 2010; Striano et al., 2012). Furthermore, during childhood, the most common EEG abnormalities are 2,5–4 Hz generalized spike and wave discharges (GSWD) (Leary et al., 2003). This pattern is usually more polymorphic and irregular that the classic 3-Hz spike-wave (Leary et al., 2003), but could be likewise similar and elicited by hyperventilation. Given this combination of EEG features and seizure type, GLUT1DS should be considered in the differential diagnosis of childhood (CAE) or juvenile absence epilepsy (JAE), particularly if atypical features are present (Byrne et al., 2011). Myoclonic-astatic and myoclonic absences epilepsy phenotypes have been also reported (Larsen et al., 2015; Mullen et al., 2011). A chronic metabolic disturbance caused by lowered glucose transport is considered to be

* Corresponding author at: Brain and Behavior Department, University of Pavia, Via Mondino, 2, 27100 Pavia, Italy.
E-mail address: pierangelo.veggiotti@unipv.it (P. Veggiotti).
[1] Equally contribution.

http://dx.doi.org/10.1016/j.nicl.2016.12.026

responsible for generalized epileptiform activities and epilepsy in patients with GLUT1 deficiency (Pascual et al., 2002; Seidner et al., 1998).

This study is the first investigation of the brain networks involved in the generation of GSWD in GLUT1DS by means of EEG co-registered with fMRI (EEG-fMRI). In particular, we aimed to isolate the BOLD correlates of GSWD in GLUT1DS with respect to the ones typically observed in GGE (Benuzzi et al., 2012; Gotman et al., 2005; Moeller et al., 2008; Li et al., 2009). This objective could be relevant for the following reasons: (a) to better understand the pathophysiology GLUT1DS; (b) to provide imaging biomarkers of the disorder that might orient the diagnosis; (c) to evaluate the mechanisms of 'generalized' SWD in a model not due to a channelopathy.

2. Materials and methods

2.1. Patients

Eighteen Italian GLUT1DS patients (mean age 19,22 years; range 6–43 years; 12 females) were enrolled from September 2012 to March 2015. The recruited subjects fulfilled the clinical criteria for diagnosis of GLUT1DS (Pearson et al., 2013) and all but one presented pathogenic mutations in *SLC2A1* gene (Table 1).

The clinical, molecular methods and genetic features of this GLUT1DS cohort have been previously described (De Giorgis et al., 2015; Gagliardi et al., 2012; Ragona et al., 2014; Veggiotti et al., 2010; Zorzi et al., 2008). Briefly, mutation analysis of all exons and intron-exon boundaries of *SLC2A1* was performed on genomic DNA by direct sequencing. Each fragment was sequenced on both strands. The effect of the newly detected *SLC2A1* mutations on protein structure or function was analyzed with the prediction programs ExPASy (http://www.expasy.org).

The mean age at diagnosis was 16,2 ± 11,1 years. Structural MRI scan (3T) was normal in all cases. All patients but 2 (#6; #18) experienced epileptic seizures (mean age of seizure onset was 34 ± 21 months). The most representative seizure's type was AS (10 out of 18 patients) followed by generalized tonic-clonic and myoclonic seizures. Notably, four patients had AS alone and one patient had myoclonic seizures without movement disorders. Eleven out of 18 GLUT1 subjects presented complex movement disorders, like ataxia, dystonia, chorea and paroxysmal exercise-induced dyskinesia. An intellectual impairment of variable degree was detected in 8 patients (according to the Diagnostic and Statistical Manual of Mental Disorders-DSM V). The rest of the sample displayed normal intellectual abilities, although for most of them the IQ was in the low range of normality. Seven out of the patients were on ketogenic diet either at different regimens alone (patients #4, #6, #11) or in combination with antiepileptic drugs (#2, #8, #10, #18).

A group of 18 patients with GGE served as control (mean age 24,88 years; range 5–48 years; 12 females). Patients were extracted from our database of GGE patients who underwent an EEG-fMRI study between April 2007–December 2013. The patients' inclusion criteria were the followings: 1) documented GSWD with AS during routinely video-EEG monitoring; 2) routine EEG showing normal background; 3) normal developmental milestones; 4) normal structural imaging on anatomic MRI at 3T. The GGE syndromes classification was obtained by two expert epileptologists after a careful revision of clinical and electrophysiological data of each patient (S.M., A.E.V.) according to the ILAE classification (1981). Table 2 summarizes the clinical and EEG findings of GGE population.

The human ethic committee of the University of Modena and Reggio Emilia approved this study and written informed consent was obtained from all the patients and from their parents if underage.

2.2. EEG with fMRI recordings and analysis

Video-EEG signals have been recorded by means of a 32 channels MRI compatible EEG recording system (Micromed, Italy). Patients were asked to rest with eyes closed and keep still. All recordings were performer in the early afternoon. Sedation was never used. After the fMRI acquisitions, both GLUT1DS and GGE patients were interviewed for discomfort or any clinical, even subjective, ictal events while scanning.

fMRI data (30 axial slices, TR/TE = 3000/50 ms) have been acquired using a 3T scanner (Philips) over three 10-min sessions (200 volumes/

Table 1
Clinical feature and genetic of GLUT1 patients.

Pt ID	Age(yrs)/sex	Age at diagnosis (yrs)	Glycorrhachia (mg/dl)	CSF/plasma glucose ratio	Protein mutation	Seizure type	Seizure onset (mo)	Sporadic/Familiar	Motor Signs	IQ	Treatment at fMRI
1	12/M	6	35	0.54	c1457delG_1 delG SPL	GTC, AS	11	S	PED, Dy	75	VPA
2	11/F	10	33	0.34	R126C	Myo, AS	30	S	PED, Dy	44	LEV, LTG, 3:1 KD
3	14/M	11	44	0.51	R223W	FS	11	S	PED, Cho	75	OXC
4	9/F	5	31	0.39	R153C	GTC, AS	12	F	A	104	1.8:1 KD
5	12/M	10	40	0.47	R458W	FS	40	F	PED, Cho	85	VPA
6	10/F	10	33	0.38	V165I	/	/	F	PED, Dy, Cho	66	3:1 KD
7	7/F	7	32	0.35	N34S	AS	24	F	/	76	ETS
8	12/F	9	34	0,38	R400C	AS, Myo	36	S	PED, Dy	50	LTG, 3:1 KD
9	6/F	5	40	0,41	not found	Myo, GTC	39	S	/	112	VPA, LTG, CLB
10	27/F	20	31	0.38	R126C	AS, FS Myo	8	S	PED, A	60	LEV, 3:1 KD
11	18/F	14	40	0.44	P36R	AS	18	S	/	53	2,5:1 KD
12	28/M	17	46	0.54	R458W	FS	60	S	PED, Dy	57	ETS
13	43/F	43	N/A	N/A	R458W	AS	72	F	/	78	–
14	40/F	29	41	0.44	V165I	AS, GTC	12	F	PED	55	VPA
15	24/F	24	N/A	N/A	V165I	AS	72	F	/	76	–
16	19/F	19	38	0,5	1166delV	AS	48	S	PED. Dy	80	LTG
17	39/M	39	42	0.43	N34S	AS	48	F	PED, Dy	75	CBZ
18	15/M	15	44	0,44	R400H	/	/	S	PED, Dy	56	VPA, 3:1 KD

Legend Table 1: M: Male; F: Female; A; Ataxia; AS: absences seizures; Cho: chorea; Dy: Dystonia; GTC: generalized tonic clonic seizures; FS: focal seizures; Myo: Myoclonic Seizures; N/A: not available; PED: paroxysmal exercise-induced dyskinesia. LEV: Levetiracetam; LTG: Lamotrigine; VPA: Valproate; ETS: Ethosuximide; CBZ: Carbamazepine; CLB: Clobazam; KD: ketogenic diet. S: sporadic; F: familiar.
Missense mutations were observed in the majority; case #1 and n #16 presented deletions. Amino acid mutations are represented by (capital) native amino acid (in one-letter code), amino acid number, and mutant amino acid. Nucleotide deletions are indicated by nucleotide number, del for deletion, nucleotide, or by native nucleotide, number, and mutant nucleotide.

Table 2
GGE population: clinical features and details of the EEG data during fMRI.

Clinical Data				GSWD during fMRI			
Pts ID	Age (years)/sex	Epilepsy syndrome	AEDs	N° events	Mean duration (sec)	Minimum Duration (sec)	Maximum Duration (sec)
1	24/F	JAE	LEV	45	3,24	1,5	5,4
2	33/F	JAE	VPA	15	3,61	0,8	6,8
3	47/M	JAE	VPA	21	3,71	2	5
4	48/F	CAE	VPA	14	4,03	1,2	6,1
5	26/M	Adult onset IGE	PB/TPM/ZNZ	12	4,99	2	7
6	37/F	JAE	LEV	19	3,91	1,6	8,1
7	14/F	JAE	VPA	16	3,18	1,1	6,9
8	23/F	Adult onset IGE	LEV	3	3,07	0,9	5
9	5/F	CAE	Naïve	5	5,20	2,2	7
10	20/F	JAE	Naïve	9	3,14	1,1	5,2
11	12/M	CAE	Naïve	5	7,29	2,2	10
12	9/F	CAE	Naïve	3	7,63	1,1	15
13	11/M	JAE	VPA	9	5,19	3,1	7,6
14	10/F	CAE	Naïve	6	5,07	2,2	6,9
15	41/F	Adult onset IGE	LEV	47	2,13	1	5
16	35/F	JAE	VPA	15	2,45	2,2	3,6
17	15/M	JME	LEV	8	3,40	2,1	4,4
18	38/M	JAE	VPA	41	3,74	1.7	6,6

Legend Table 2: M: Male; F: Female; JAE: juvenile absence epilepsy; CAE: childhood absence epilepsy; GGE: genetic generalized epilepsy; JME: juvenile myoclonic epilepsy; AEDs: anti-epileptic drugs; VPA: valproate; LEV: levetiracetam; PB: phenobarbital; TPM: topiramate; ZNZ: zonisamide; GSWD: generalized spike-wave discharge.

session) with continuous simultaneous Video-EEG recording. A high-resolution T1-weighted anatomical image was obtained for anatomical reference (170 sagittal slices, TR/TE = 9.9/4.6 ms).

After offline correction of the gradient artifacts and filtering of the EEG signal (Allen et al., 2000), the EEG data were reviewed and pre-processed according to our previous published method (Avanzini et al., 2014; Ruggieri et al., 2015). Two experienced electroencephalographers reviewed the pre-processed EEG recordings independently (A.R., P.V.) in order to identify GSWD. After identification, epileptiform activities were manually marked on EEG and exported as single event or variable-length blocks depending on their duration observed by EEG.

The Matlab 7.1 and SPM8 (http://www.fil.ion.ucl.ac.uk/spm/) software was used for data analysis. All functional volumes were slice time corrected, realigned to the first volume acquired, spatial normalized and smoothed with $8 \times 8 \times 8$ mm full-width half maximum Gaussian Kernel. Movement artifacts individuated by analysis of Video-EEG recordings (blinking, lip smacking, swallowing, head movements) were considered as confounders in the model and treated as stick functions or blocks as appropriated (Ruggieri et al., 2015). In addition, 24 realignment parameters [six scan realignments parameters from image pre-processing and a Volterra expansion of these (Friston et al., 1996)] were included in the model as confounds.

2.2.1. First level analysis

Maps of the t-statistic were created using the timing of the GSWD as events (stick functions or blocks) within the General Liner Model (GLM) framework. In case of blocks, the duration of GSWD was specified. All regressors were convolved with the canonical hemodynamic response function (HRF) plus its temporal and dispersion derivatives (Lemieux et al., 2008).

2.2.2. Group level analysis

The effect of GSWD at the group level was tested for GLUT1DS and GGE patients separately by means of the fixed-effect or the random approach as appropriate (Friston et al., 1999). When using the fixed-effect model, a conjunction analysis of the BOLD increases and decreases effects for all the subjects was done with global null hypothesis, to evaluate whether the selected congruent contrasts were consistently high and jointly significant (Friston et al., 1999). For the random effect analysis, a full factorial design was used to test for within effects (1-way analysis of variance [ANOVA]) with 1 group of patients (18 GGE) and three basis functions (canonical HRF and its derivatives) as factors. Group analysis results were considered significant at the $p < 0.05$ corrected for FWE or, if any results were revealed, a less conservative statistical inference was considered ($p < 0.001$, uncorrected). In these cases, an additional threshold of 5-voxels extent was applied in order to discard BOLD changes occurring in scattered voxels. The fMRI t-maps were superimposed on the canonical T1-weighted images as implemented in SPM8.

Subsequently, we compared the BOLD changes obtained in the two populations in order to isolate the GSWD-related hemodynamic patterns specific of the two epileptic conditions. To this end, 10 age and sex matched GGE patients were extracted from the whole GGE sample (patient #7, #9, #10, #11, #12, #13, #14, #15, #17, #18). Within this subgroup, a total number of 149 GSWD were recorded (mean duration 4,59 s). A single fixed effect analysis that included both groups in one matrix (10 GLUT1DS and 10 GGE) was performed. The GSWD effect across the 10 GGE patients was obtained using fixed effect approach with conjunction analysis (Friston et al., 1999) similar to what previously described for GLUT1DS. Further, we explored the differences by applying an exclusive masking procedure between the conjunction contrasts each related to the specific patients' populations. In details, to isolate the brain regions that were significantly involved in the main effect "GSWD > baseline" in GLUT1DS population but not in the main effect "GSWD > baseline" in GGE, the conjunction contrast "GSWD > baseline" in GLUT1DS was exclusively masked by the mask conjunction contrast "GSWD > baseline" in GGE. By counterpart, to isolate the brain regions exclusively activated by GSWD in GGE, the conjunction contrast "GSWD > baseline" in GGE was exclusively masked by the conjunction contrast "GSWD > baseline" in GLUT1DS. SPM exclusive masks were thresholded at $p < 0.05$ uncorrected, whereas the contrasts to be masked were thresholded at $p < 0.001$. In this way, those voxels that reached a level of significance at $p < 0.05$ in the mask contrast were excluded from the analysis.

Finally, for the GLUT1DS patient group only, we performed additional whole brain second-level correlations analyses between the contrast (GSWD) and the main clinical measurements including: age (years); age at seizure onset (months); total IQ; glycorrhachia values (mg/dl) and the CSF/plasma glucose ratio at the time of diagnostic workup. We also explored the effect of the ketogenic diet (KD) on the GSWD-related BOLD changes. Indeed, five GLUT1DS patients (#6, #8, #10, #11, #18) were on KD (alone or with antiepileptic treatment-AED) (KD+) at the time of the fMRI study, while the remaining were naïve (#13) or only under AED (#3, #5, #9, #17) (KD-). In a separate analysis, we have performed a conjunction analysis, based on the fixed effect model, of the GSWD-related T contrast in the KD+ subgroup and then

we compared this effect with the one obtained in KD-. The differences were explored by applying an exclusive masking procedure at a threshold of $p < 0.05$, uncorrected for multiple comparisons.

3. Results

3.1. EEG findings during fMRI

In GGE, EEG during fMRI shown symmetric and synchronous generalized 3–4 Hz SWD in all the patients. A total of 293 events (mean of 17 events per subject) were acquired, from a minimum of three GSWD in subject #8 and #12, to a maximum of 47 events in subject #15. The duration of GSWD ranged from 1 s to 15 s, with a mean duration across subjects of 4.2 s (see Table 2). The GSWD occurrence was not accompanied by clinical manifestations, even subjective, in any patients.

In GLUT1DS, EEG during fMRI revealed SWD in 10 subjects. Six patients (#3, #5, #6, #9, #11, #17) presented 3–4 Hz diffuse spike-and-waves discharges; four patients showed more focal discharges over the bilateral frontal leads (#8, #10, #13, #18). A total number of 152 SWD were recorded (range: 6–28). The duration of GSWD ranged from 1 s to 18 s, with a mean duration across GLUT1DS of 4,31 s (see Table 3). Fig. 1, panel A shows the EEG pattern in a representative case (#10). The GLUT1DS patients did not shown any clinical seizures, even subtle or subjective, during the EEG-fMRI. In addition, no persistent or paroxysmal movement disorders (dystonia, dyskinesia, chorea) were recorded during the experimental sessions.

For both GLUT1DS and GGE populations, the absence of clinical events (seizure and movement disorder) was verified by either the inspection of the Video recorded simultaneously during fMRI acquisitions and the post-scanning individual patient's interview.

3.2. GSWD related BOLD changes in GLUT1DS

Table 3 summarizes the fMRI findings at single subject level. GSWD-related hemodynamic changes were distributed homogenously across patients, revealing the involvement of the same cortico(frontal)-subcortical(basal ganglia) network. In particular, all GLUT1DS demonstrated BOLD changes at a frontal network, encompassing premotor (prefrontal cortex, supplementary motor area-SMA, cingulate cortex) (9 patients) and motor brain regions (5 subjects). The frontal BOLD response was positive in all the cases except four patients (#6, #8, #13, #18). Subcortical positive hemodynamic changes were mainly confined at the basal ganglia (putamen) (5 patients) while only one patient (#13) demonstrated thalamic BOLD signal increases. Finally, 7 GLUT1DS demonstrated significant BOLD responses at the posterior part of the Default Mode Network, essentially as signal increases (6 subjects). Fig. 1, panel B shows the GSWD-related fMRI map in a representative case (#10).

At the group-level, fixed effect analysis ($p < 0.05$ corrected for FWE) showed BOLD positive changes over the bilateral premotor cortex (global maxima-GM) (Brodmann Area-BA9), precuneus (BA7), inferior frontal gyrus (BA46) and SMA (BA6), while decreases involved the bilateral motor cortex (BA2) and the pericentral lobule (BA5) (Fig. 2A). At a less conservative threshold ($p < 0.001$ uncorrected) a bilateral thalamic deactivation was detected. The conjunction analysis ($p < 0.001$ uncorrected) revealed commonalities in BOLD signal increases between the ten subjects in the bilateral premotor cortex (GM) and right putamen; negative BOLD changes were detected in the thalamus, primary motor cortex, inferior frontal gyrus. The BOLD increase in the premotor cortex survived at a more conservative threshold ($p < 0.05$ corrected for FWE) (Fig. 2B).

3.3. GSWD-related BOLD changes in GGE

At the group level (n. of patients = 18), random effect analysis ($p < 0.05$ corrected for FWE) revealed BOLD signal increases in the bilateral thalami (GM) and cerebellum, while negative changes were observed in the posterior part of the Default Mode Network (DMN) encompassing the bilateral precuneus (BA7), and inferior parietal lobule (BA40) (Supplementary Fig. 1). When the analysis was limited to 10 GGE, the conjunction approach based on the fixed-effect model

Table 3
EEG and fMRI results at single-subject level.

PT ID	ED				Bold changes							
	Type and location	Number/mean duration (sec)	Minimum duration (sec)	Maximum duration (sec)	Basal Ganglia	Frontal operculum	Premotor cortex	SMA	Cingulate cortex	Pericentral cortex	DMN**	Other
Pt3	B F SWD	12/11,89	2,68	18,1	B (>R) (3.51) (i)	B (>L) (4.94) (i)	B (>R) (5.07) (i)	L (4.50) (i)	–	–	L (4.90) (i)	–
Pt5	Diffuse SWD	6/2,1	1	3.24	–	B(>R) (4.82) (i)	R (4.88) (i)	–	–	–	–	–
Pt6	Diffuse SWD	12/2,17	0,36	4,53	B (>L) (2.58) (i)	–		L (3.46) (d)*	B (>L) (2.89) (d)*	B (>L) (3.82) (d)*	–	B cerebellum (2.99) (d)*
Pt8	B F SWD (>L)	11/2,14	0	4.01	–	–		R (d)*	–	–	–	–
Pt9	Diffuse SWD	15/3,2	0	15.24	L (2.72) (i)*	–	R (4.35) (i)	L (3.02) (i)*	–	B (>R) (3.75) (i)*	B (>R) (4.30) (i)*	B cerebellum (4.32) (i)
Pt10	B F SWD	18/4,28	1	17,84	B (>L) (4.86) (i)	B(>L) (3.99) (i)	B (>R) (>7.59) (i)	B (>L) (>7.59) (i)	L (>7.59) (i)	B (>L) (6.35) (i)	L (5.07) (i)	–
Pt11	Diffuse SWD	15/1,34	0	2,05	–	B (4.92) (i)	–	B (4.94) (i)	–	–	B (6.15) (i)	–
Pt13	B F SWD	28/3,6	0	15,8	L (3.82) (i)*	B (>R) (5.67) (d)		B (>R) (6.41) (d)		B (>R) (7.81) (d)	B (>L) (7.81) (d)	B thalamus (4.40) (i)* B cerebellum (4.12) (i)*
Pt17	Diffuse SWD	10/3	1	4,5	–	–		–	–	B (>R) (3.32) (i)*	B (>R) (3.17) (i)*	L TP junction (i)
Pt18	B F SWD	25/3,5	1	8,4	–	–	B (5.39) (d)	–	–	–	R (3.77) (i)*	–

Legend Table 3: FMRI results are displayed using a threshold set at $p < 0.05$ corrected for FWE and $p < 0.001$ uncorrected if no BOLD changes were detected at the more conservative statistical inference (the results obtained using a $p < 0.001$ uncorrected are indicated by the asterisk [*]). The numbers in brackets indicate the maximal t-values. ED: epileptic discharges; SW: Slow Waves; SWD: spike-wave discharges; L: Left; R: Right; B: Bilateral; F: Frontal; TP: Temporo-Parietal. (i) increase BOLD signal; (d) decrease BOLD signal; L: Left; R: Right; B: Bilateral; SMA: Supplementary Motor Area; **DMNp: Default-mode Mode Network which includes: posterior part of DMN (precuneus/posterior cingulate, bilateral inferior parietal lobuli).

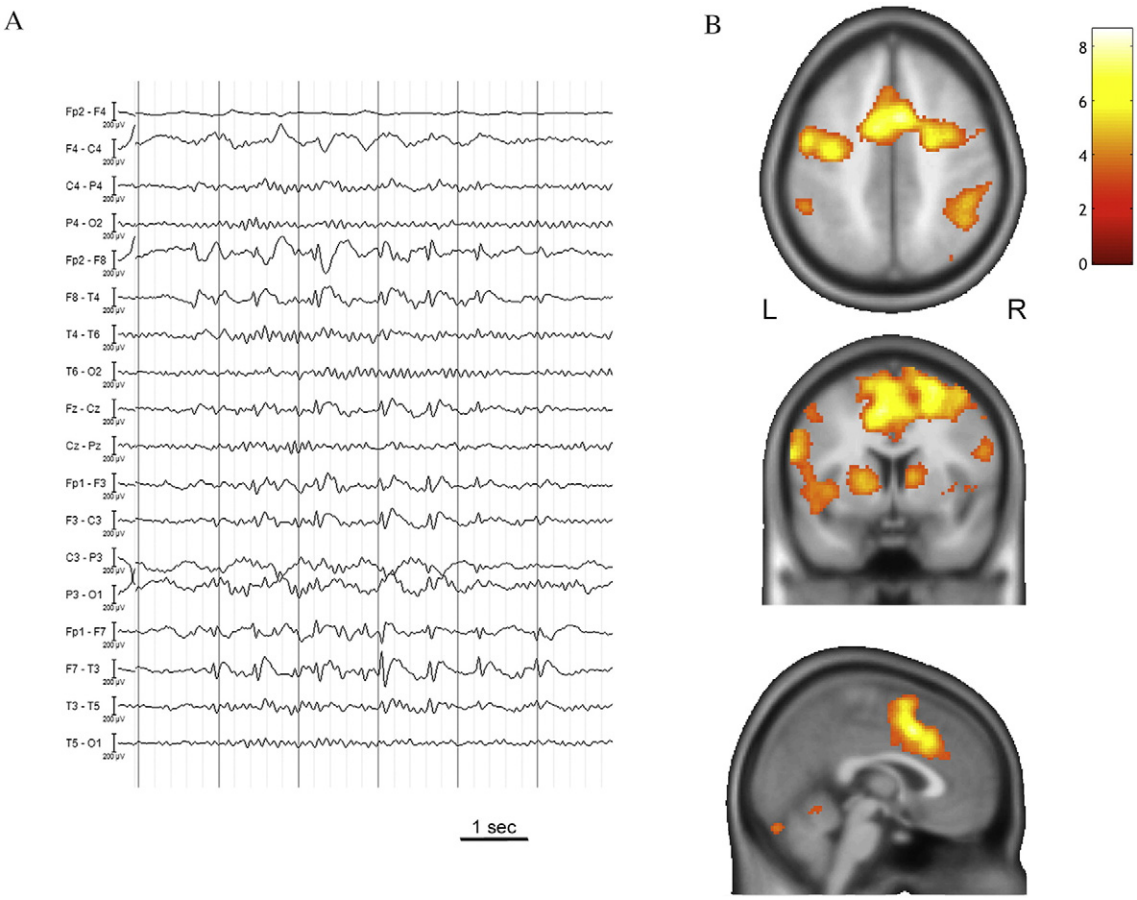

Fig. 1. EEG-fMRI results in a representative GLUT1 patient. *Panel A*: Representative EEG recorded during fMRI acquisition in patients #10. The EEG is displayed in bipolar montage after gradient and pulse artifact correction. Note the burst of 1.5–2 Hz SWD over the bilateral frontal fields. *Panel B*: fMRI results ($p < 0.05$ corrected for FWE) overlaid to the canonical T1 image, axial, coronal and sagittal slice. Significant BOLD signal increases were detected at the bilateral middle frontal gyrus (global maxima) (BA6), supplementary Motor Area (SMA) (BA6), putamen, post-central cortex (BA40), inferior frontal gyrus (BA9), left anterior cingulate cortex (BA32), left precuneus (BA19). No BOLD decreases were detected. R = Right; L = Left; BA: Brodmann Area.

revealed commonalities in BOLD signal increases in the bilateral thalami (more right) and cerebellum.

3.4. GLUT1 versus GGE

GLUT1DS patients demonstrated during GSWD increased neuronal activity in the bilateral putamen, precuneus, middle cingulate cortex, right SMA and right paracentral lobule, while GGE do not (Fig. 3A). On the contrary, no GGE-exclusive GSWD-BOLD correlates were observed at the considered threshold.

3.5. Correlations between BOLD signal and clinical measures

Whole-brain correlation analyses using individual clinical characteristics of the GLUT1DS patients disclosed a linear positive relationship between the interictal discharges - related BOLD changes and the levels of glycorrhachia (and also CSF/plasma glucose ratio) over a bilateral cortical network including the opercular-insular cortex, the post-central cortex and superior parietal lobuli (Fig. 3B). No significant correlations were discovered with the age, age at seizure onset, and the total IQ. The conjunction analysis limited to KD + patients ($p < 0.001$, uncorrected for FWE) demonstrated common BOLD positive responses over the bilateral precuneus, bilateral inferior parietal lobule, right precentral gyrus and a small spot in the left putamen (data not shown). No negative responses were detected. The comparison between the hemodynamic changes in GLUT1DS KD + versus KD-, did not isolated any BOLD cluster specific of GLUT1DS KD + and viceversa, at the considered threshold.

4. Discussion

This work represents the first attempt to investigate the hemodynamic correlates of interictal epileptiform activity (IED) in a cohort of patients with GLUT1DS. To note, previous functional neuroimaging studies in these patients (Akman et al., 2015; Pascual et al., 2002, 2007; Suls et al., 2008) were unable to obtain the EEG recordings at the time of imaging and the interictal/ictal state was assessed only by clinical inspection. In our study, the video-EEG recorded simultaneously during fMRI acquisitions allowed both to record the cerebral brain activity and to exclude the presence of any clinical seizure as well as paroxysmal movement disorder during the experimental sessions. Consequently, the resulted maps represent a real-time picture of brain function during IED in GLUT1DS.

The studied population is representative of the complex phenotypical spectrum of the disorder and particularly with early onset absence seizures as the main seizure type (Arsov et al., 2012b; Byrne et al., 2011; Leary et al., 2003; Striano et al., 2012; Wang et al., 2005) and paroxysmal exertion-induced dystonia (PED) as most frequent movement disorder (Suls et al., 2008). However, epilepsy and motor signs were not homogenously distributed across patients as well as treatment and age at the time of the fMRI study. This heterogeneous presentation reflects the intrinsic and natural variability of the syndrome, as largely documented (Brockmann, 2009; De

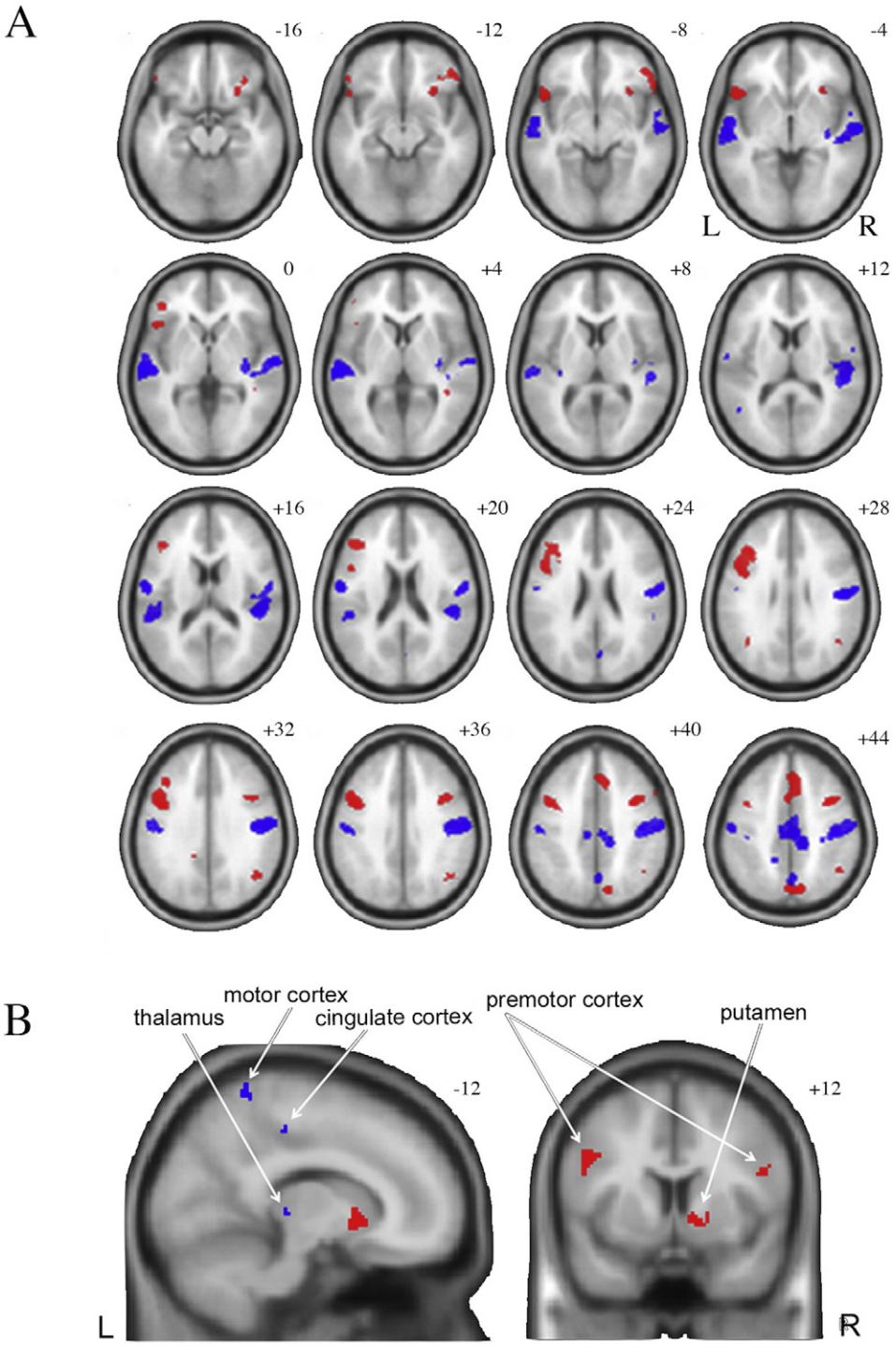

Fig. 2. Results of SWD-related second level analysis in GLUT1DS. *Panel A*: FFX {T} BOLD signal changes across the 10 GLUT1DS with recorded SWD. Positive (in red) and negative (in blue) BOLD responses are displayed onto the T1-canonical image, axial slices ($p < 0.05$ corrected for FWE). See text for a description of positive and negative BOLD correlations. *Panel B*: Conjunction analysis results ($p < 0.001$, uncorrected) shown common areas of positive and negative BOLD correlation with the SWD across the 10 GLUT1DS subjects. L = Left; R = Right.

Giorgis and Veggiotti, 2013; De Giorgis et al., 2015; Verrotti et al., 2012). The clinical variability of GLUT1DS represents a difficulty to diagnose the disorder, especially for patients with mild or non-classical phenotype, who are likely to be under-diagnosed (Brockmann, 2009; De Giorgis et al., 2015). In this contest, the present work might be of importance to underlie the pathophysiological fingerprints of this metabolic encephalopathy.

As far as the fMRI analyses, the results of our work are innovative for two main aspects. Firstly, the observed BOLD findings allowed delineating a well-defined network of cortical-subcortical regions that are involved in the generation of GSWD in GLUT1DS. The results at the second level analysis showed an increase BOLD signal, and hence an increased neuronal activity, in the premotor-striatal network (bilateral premotor cortex, SMA, anterior cingulate and basal ganglia) and a simultaneous reduced metabolic demand of the motor cortex and thalamus. Notably, the analysis of single-subject GSWD-related BOLD changes was consistent with the group results as most of the patients showed significant BOLD changes within the premotor-basal ganglia circuit (see Table 3). The altered metabolism of thalamus and cortico-striatal pathways found in our patients speaks to the severe abnormality

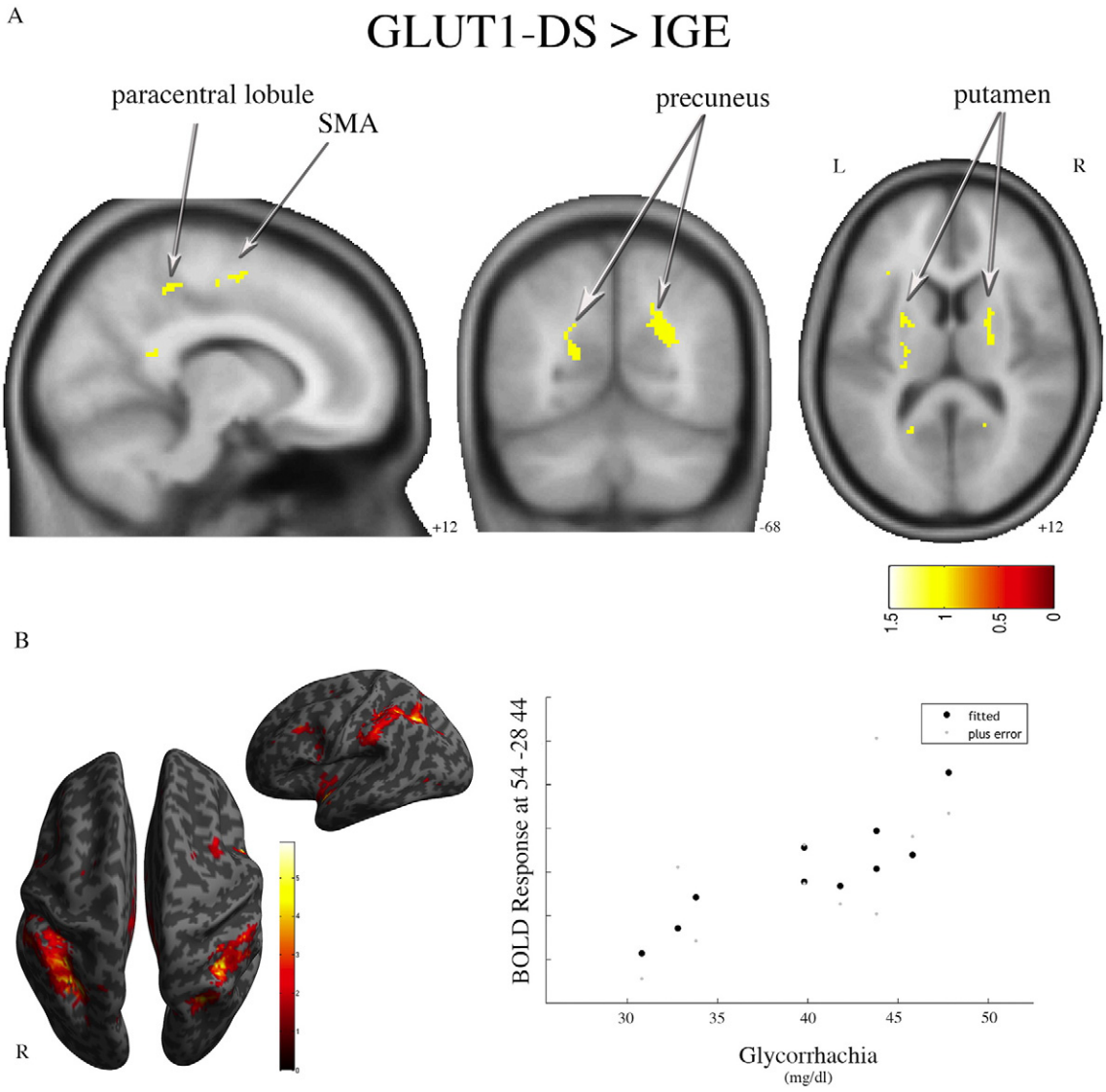

Fig. 3. Specific BOLD response to GSWD in GLUT1DS and correlation with clinical variables. *Panel A*: the main effect conjunction contrast "GSWD > baseline" in GLUT1DS was exclusively masked by the mask conjunction contrast "GSWD > baseline" in GGE, at a threshold of $p < 0.05$, uncorrected for multiple comparison. GSWD-related BOLD signal increases specific to GLUT1DS were detected at the bilateral putamen, precuneus (BA31), middle cingulate cortex (BA32), SMA (BA6) and right paracentral lobule (BA5). Clusters of activation are overlaid on the canonical T1-weighted structural scan. *Panel B:* A linear correlation between BOLD changes and levels of glycorrhachia is evident in GLUT1DS. The results are displayed onto canonical render images ($p < 0.001$, uncorrected). The graph demonstrated the positive correlation between the two variables (right image). L = Left; R = Right, BA: Brodmann Area.

of this functional system and leads us to hypothesize that it constitutes the central epileptogenic substrate in GLUT1DS.

As second main result, our findings shown that the BOLD dynamics related to GSWD in GLUT1DS are substantially different from the BOLD correlates of GSWD in typical genetic generalized epilepsies (Aghakhani et al., 2004; Benuzzi et al., 2012; Carney et al., 2010; Gotman et al., 2005; Hamandi et al., 2006; Li et al., 2009; Moeller et al., 2010; Vaudano et al., 2009), reinforcing the hypothesis of a specific relationship with the GLUT1DS disorder. Intriguingly, the cortical networks observed in GLUT1DS patients are very similar to the one described, by means of EEG-fMRI, in patients with 'Doose syndrome' or Myoclonic Astatic Epilepsy (MAE) (Moeller et al., 2014). This commonality is of particular interest since MAE has been reported as one of the possible phenotypes of GLUT1DS (Mullen et al., 2011). With respect to the BOLD findings previously reported in MAE (Moeller et al., 2014), and more in general to GGE sub-syndromes, our GLUT1 population didn't show any increase in BOLD signal at thalamic level and no decreases in the Default Mode Network (DMN) at a group level. By contrast, GLUT1DS revealed bilateral activation in the putamen and different premotor and parietal areas (Fig. 3A); this pattern in not generally reported in GGE, except for single cases description (see Carney and Jackson, 2014 as review). The consistency of 3–4 Hz GSWD associated hemodynamic changes in GGE across studies, further support that the mechanisms subserving GSWD generation in GLUT1DS involve different neural dynamics. The irregular and slower phenotype of GSWD in GLUT1DS might partially explain these BOLD differences. Nevertheless, previous evidences failed to detect specific hemodynamic pattern linked to different GGE subgroups, independently to the morphology and length of GSWD (Pugnaghi et al., 2014).

The revealed hemodynamic changes in GLUT1DS are concordant with findings observed by means of positron emission tomography (PET) imaging in humans (Akman et al., 2015; Pascual et al., 2002–2007; Suls et al., 2008). Overall considered, interictal ^{18}F-fluorodeoxyglucose PET demonstrated a relatively homogeneous pattern with glucose hypometabolism in the mesial temporal regions, pre-postcentral gyrus, premotor cortex, inferior parietal lobule and thalamus, and a relative increased in the basal ganglia (putamen). These PET findings demonstrated to be stereotyped regardless of disease severity, or type and duration of therapy, and persist into adulthood (Pascual et al., 2002–2007). In other words, hypometabolism pattern may not

show a progressive changes with increasing age or clinical course of seizures (Akman et al., 2015). This argument is concordant with our fMRI findings, as similar BOLD patterns were observed in adults and children and no relationship has been detected between age and IED-related hemodynamic changes. To note, we observed that BOLD signal related to epileptic discharges at the time of fMRI correlated with the level of CSF glucose at the time of diagnosis (Fig. 3B). This means that the lower the CSF glucose in early childhood, the lower are the BOLD signal changes IED-related, several years later at the time of the imaging study. Such linear correlation is particularly evident at the bilateral sensory-motor and parietal circuits which neuronal activity is highly dependent to the glucose supply especially in early infancy (Chugani, 1998). This finding supports the observations of Akman et al. (2015) who suggested "that brain glucose hypometabolism, present in infancy, leaves an imprint that persists even when the precipitating condition causing the hypoglycorrachia is corrected". Probably, hypoglycorrachia during a vulnerable period in early infancy can affect the maturation of the developing striatal-thalamo-cortical networks and synaptic connections, leaving a persistent alteration even when hypoglycorrhachia is corrected. As far as the correlation between the GSWD-related BOLD changes and other clinical variables, no relationship was detected with the type of treatment, particularly in relation to the presence/absence of KD (KD + versus KD-). Such inconclusive result needs to be taken with caution given the low number of patients in each subgroup. A further dedicated study on a larger cohort of GLUT1DS patients with IED during fMRI scanning and different treatments (KD and/or AED) needs to be performed to test the specific effect of KD on the brain networks function in GLUT1DS.

Our fMRI results demonstrated that the disrupted metabolism of the premotor-basal ganglia circuit is responsible for the generation and maintenance of interictal GSWD. Since we did not record any clinical seizure as well as involuntary movements during the experimental sessions, we could not directly link the detected hemodynamic changes with these clinical phenomena. Previous attempts to segregate the PET patterns based on the GLUT1DS clinical phenotype shown that a prominent hypometabolism in the thalamus and mesial temporal cortex linked to the presence of epilepsy (Akman et al., 2015) while PED frequency score was positively correlated to the metabolic activity of basal ganglia (putamen), and negatively with the premotor cortex (anterior cingulate and superior frontal cortex) (Suls et al., 2008). Intriguingly, ictal SPECT during a PED episode shown hyper-perfusion over the motor cortex and putamen (Suls et al., 2008). Based on these observations, a dysfunction of the cortico-striatal pathways has been postulated to play a role in the pathophysiology of PED (Suls et al., 2008). Our fMRI maps appear to support this hypothesis as most of our patients shown PED as the main motor disorder. It is likely that an altered excitability of striatal-thalamo-(frontal)cortical pathway, which is the consequence of a defect in glucose transport across the blood-brain barrier, subserves the generation of both epileptic activity and PED. Given the lack of movement disorders during fMRI, this conclusion remains speculative and warrants further investigations to be confirmed.

The pathogenic role of low CSF glucose to determine GLUT1DS phenotype, including seizures, has been objected of intense speculations (Arsov et al., 2012a, 2012b). The primary mechanism in GLUT1 deficiency seems represented by a reduced substrate delivery rather than altered membrane excitability as observed in channelopathies (Arsov et al., 2012a, 2012b). Furthermore, most likely, there is reduced availability of interstitial medium glucose to both astrocytes and neurons, the former of which rely on GLUT1 for their glucose uptake, unlike neurons that utilize the transporter GLUT3 (Vannucci et al., 1997). Thus, the astroglial glucose uptake is severely compromised being restricted by its failure at both the blood-brain barrier and the cellular membrane. This astroglial failure could result in a decrease in the amount of lactate produced for subsequent delivery to the neuron (Pellerin and Magistretti, 2004) resulting in downstream neuronal dysfunction. An early effect of this pathogenic mechanism on the structures that first start to mature, like thalamus, might constitute the basis of the epileptiform abnormalities in neuroglycopenia (Giaume et al., 2010). An altered thalamic function, indeed, might affect the cortico-thalamic and thalamo-cortical oscillatory networks, leading to synchronized spike-and-wave discharges (Jones, 2001; McCormick and Contreras, 2001). In line with this proposed mechanism, our findings indicate an opposite BOLD response in the thalamus (negative change) and cortico-striatal circuit (positive change). We might hypothesize that the reduced metabolic activity of the thalamic regions leads to a change in the activity of the connected cortico-striatal areas, resulting in their reduced inhibition and hence hyper-excitation. Certainly, given the limited sample of patients investigated, further studies are needed to replicate our findings on a larger cohort of GLUT1DS subjects.

4.1. Study limitations

The major limitation of this study is related to the number of the investigated subjects, which is justified by the rarity of this genetic disorder. This limitation might lead to caution in generalizing the results outside of the group of subjects analyzed. The fixed effect approach applied within the GLUT1DS cohort and between the GLUT1DS and GGE, allows to make a comment about the specific subjects studied (only those) but it cannot be used to obtain an inference at the population level. However, by using a conjunction approach, based on the fixed-effect model, we were able to infer that at least some proportion of the population from which the patients came show this effect (Friston et al., 1999), i.e. to extend our speculations to the general GLUT1DS population.

4.2. Conclusions

In conclusion, our study provides new findings on the epileptic networks subserving epilepsy in GLUT1 deficiency syndrome. Several question, however, are unanswered and should be addressed by future studies investigating both microstructural abnormalities in GLUT1 patients with milder form of the disease, as well as the integrity or alteration of resting-state networks subserving motor and cognitive functions.

Supplementary data to this article can be found online at http://dx.doi.org/10.1016/j.nicl.2016.12.026.

Fundings

A.E. Vaudano received research grant support from the Fondazione Epilessia LICE (Lega Italiana contro L'Epilessia) Onlus, and from research grant support from the Ministry of Health (MOH), Regione Emilia Romagna, grant ID RPRUA1GR-2013-00000120. S. Olivotto received research grant support from AIEF (Associazione Italiana Epilessia Farmacoresistente) Onlus. A. Ruggieri received a PhD bursary from the University of Modena and Reggio Emilia. V. De Giorgis received a PhD bursary from the University of Pavia. P. Veggiotti received educational grant from EISAI S. Meletti received Research grant support from the Ministry of Health (MOH), grant ID NET-2013-02355313-3; from the non-profit organization CarisMO Foundation, grant ID A.010@FCRMO RINT@MELFONINFO; has received personal compensation as scientific advisory board member for UCB and EISAI. Other authors report no disclosures. The authors have stated that they had no interests that might be perceived as posing a conflict or bias.

References

Aghakhani, Y., Bagshaw, A.P., Bénar, C.G., Hawco, C., Andermann, F., Dubeau, F., Gotman, J., 2004. fMRI activation during spike and wave discharges in idiopathic generalized epilepsy. Brain 127, 1127–1144.

Akman, C.I., Provenzano, F., Wang, D., Engelstad, K., Hinton, V., Yu, J., Tikofsky, R., Ichese, M., De Vivo, D.C., 2015. Topography of brain glucose hypometabolism and epileptic network in glucose transporter 1 deficiency. Epilepsy Res. 110, 206–215.

Allen, P.J., Josephs, O., Turner, R., 2000. A method for removing imaging artifact from continuous EEG recorded during functional MRI. Neuroimage 12, 230–239.
Arsov, T., Mullen, S.A., Rogers, S., Phillips, A.M., Lawrence, K.M., Damiano, J.A., Goldberg-Stern, H., Afawi, Z., Kivity, S., Trager, C., Petrou, S., Berkovic, S.F., Scheffer, I.E., 2012a. Glucose transporter 1 deficiency in the idiopathic generalized epilepsies. Ann. Neurol. 72, 807–815.
Arsov, T., Mullen, S.A., Damiano, J.A., Lawrence, K.M., Huh, L.L., Nolan, M., Young, H., Thouin, A., Dahl, H.H., Berkovic, S.F., Crompton, D.E., Sadleir, L.G., Scheffer, I.E., 2012b. Early onset absence epilepsy: 1 in 10 cases is caused by GLUT1 deficiency. Epilepsia 53, e204–e207.
Avanzini, P., Vaudano, A.E., Vignoli, A., Ruggieri, A., Benuzzi, F., Darra, F., Mastrangelo, M., Dalla Bernardina, B., Nichelli, P.F., Canevini, M.P., Meletti, S., 2014. Low frequency mu-like activity characterizes cortical rhythms in epilepsy due to ring chromosome 20. Clin. Neurophysiol. 125 (2), 239–249.
Benuzzi, F., Mirandola, L., Pugnaghi, M., Farinelli, V., Tassinari, C.A., Capovilla, G., Cantalupo, G., Beccaria, F., Nichelli, P., Meletti, S., 2012. Increased cortical BOLD signal anticipates generalized spike and wave discharges in adolescents and adults with idiopathic generalized epilepsies. Epilepsia 53 (4), 622–630.
Brockmann, K., 2009. The expanding phenotype of GLUT1-deficiency syndrome. Brain and Development 31 (7), 545–552.
Byrne, S., Kearns, J., Carolan, R., Mc Menamin, J., Klepper, J., Webb, D., 2011. Refractory absence epilepsy associated with GLUT-1 deficiency syndrome. Epilepsia 52 (5), 1021–1024.
Carney, P.W., Jackson, G.D., 2014. Insights into the mechanisms of absence seizure generation provided by EEG with functional MRI. Front. Neurol. 5, 162.
Carney, P.W., Masterton, R.A., Harvey, A.S., Scheffer, I.E., Berkovic, S.F., Jackson, G.D., 2010. The core network in absence epilepsy: differences in cortical and thalamic BOLD response. Neurology 75, 904–911.
Commission on Classification and Terminology of the International League Against Epilepsy, 1981. Proposal for revised clinical and electrographic classification of epileptic seizures. Epilepsia 22, 489–501.
Chugani, H.T., 1998. A critical period of brain development: studies of cerebral glucose utilization with PET. Prev. Med. 27 (2), 184–188.
De Giorgis, V., Veggiotti, P., 2013. GLUT1 deficiency syndrome 2013: current state of the art. Seizure 22 (10), 803–811.
De Giorgis, V., Teutonico, F., Cereda, C., Balottin, U., Bianchi, M., Giordano, L., Olivotto, S., Ragona, F., Tagliabue, A., Zorzi, G., Nardocci, N., Veggiotti, P., 2015. Sporadic and familial glut1ds Italian patients: a wide clinical variability. Seizure 24, 28–32.
De Vivo, D.C., Trifiletti, R.R., Jacobson, R.I., Ronen, G.M., Behmand, R.A., Harik, S.I., 1991. Defective glucose transport across the blood-brain barrier as a cause of persistent hypoglycorrhachia, seizures, and developmental delay. N. Engl. J. Med. 325, 703–709.
Friston, K.J., Williams, S., Howard, R., Frackowiak, R.S., Turner, R., 1996. Movement-related effects in fMRI time-series. Magn. Reson. Med. 35 (3), 346–355.
Friston, K.J., Holmes, A.P., Price, C.J., Büchel, C., Worsley, K.J., 1999. Multisubject fMRI studies and conjunction analyses. NeuroImage 10, 385–396.
Gagliardi, S., Davin, A., Ricca, I., Grieco, G.S., Zangaglia, R., Pierelli, F., Ghiroldi, A., Pacchetti, C., Casali, C., Cereda, C., 2012. A new GLUT-1 mutation in a family with glucose transporter 1 deficiency syndrome. Mov. Disord. 27 (6), 804–805.
Giaume, C., Koulakoff, A., Roux, L., Holcman, D., Rouach, N., 2010. Astroglial networks: a step further in neuroglial and gliovascular interactions. Nat. Rev. Neurosci. 11 (2), 87–99.
Gotman, J., Grova, C., Bagshaw, A., Kobayashi, E., Aghakhani, Y., Dubeau, F., 2005. Generalized epileptic discharges show thalamocortical activation and suspension of the default state of the brain. Proc. Natl. Acad. Sci. U. S. A. 18 (102(42)), 15236–15240.
Hamandi, K., Salek-Haddadi, A., Laufs, H., Liston, A., Friston, K., Fish, D.R., Duncan, J.S., Lemieux, L., 2006. EEG-fMRI of idiopathic and secondarily generalized epilepsies. NeuroImage 31 (4), 1700–1710.
Jones, E.G., 2001. The thalamic matrix and thalamocortical synchrony. Trends Neurosci. 24, 595–601.
Larsen, J., Johannesen, K.M., Ek, J., Tang, S., Marini, C., Blichfeldt, S., Kibaek, M., von Spiczak, S., Weckhuysen, S., Frangu, M., Neubauer, B.A., Uldall, P., Striano, P., Zara, F., MAE working group of Euro EPINOMICS RES Consortium, Kleiss, R., Simpson, M., Muhle, H., Nikanorova, M., Jepsen, B., Tommerup, N., Stephani, U., Guerrini, R., Duno, M., Hjalgrim, H., Pal, D., Helbig, I., Møller, R., 2015. The role of SLC2A1 mutations in myoclonic astatic epilepsy and absence epilepsy, and the estimated frequency of GLUT1 deficiency syndrome. Epilepsia 56, e203–e208.
Leary, L.D., Wang, D., Nordli Jr, D.R., Engelstad, K., De Vivo, D.C., 2003. Seizure characterization and electroencephalographic features in Glut-1 deficiency syndrome. Epilepsia 44, 701–707.
Lemieux, L., Laufs, H., Carmichael, D., Paul, J.S., Walker, M.C., Duncan, J.S., 2008. Noncanonical spike-related BOLD responses in focal epilepsy. Hum. Brain. Mapp. 29 (3), 329–345.
Li, Q., Luo, C., Yang, T., Yao, Z., He, L., Liu, L., Xu, H., Gong, Q., Yao, D., Zhou, D., 2009. EEG-fMRI study on the interictal and ictal generalized spike-wave discharges in patients with childhood absence epilepsy. Epilepsy Res. 87 (2–3), 160–168.
McCormick, D.A., Contreras, D., 2001. On the cellular and network bases of epileptic seizures. Annu. Rev. Physiol. 63, 815–846.
Moeller, F., Siebner, H.R., Wolff, S., Muhle, H., Granert, O., Jansen, O., Stephani, U., Siniatchkin, M., 2008. Simultaneous EEG-fMRI in drug-naive children with newly diagnosed absence epilepsy. Epilepsia 49 (9), 1510–1519.
Moeller, F., LeVan, P., Muhle, H., Stephani, U., Dubeau, F., Siniatchkin, M., Gotman, J., 2010. Absence seizures: individual patterns revealed by EEG-fMRI. Epilepsia 51, 2000–2010.
Moeller, F., Groening, K., Moehring, J., Muhle, H., Wolff, S., Jansen, O., Stephani, U., Siniatchkin, M., 2014. EEG-fMRI in myoclonic astatic epilepsy (Doose syndrome). Neurology 82, 1508–1513.
Mullen, S.A., Suls, A., De Jonghe, P., Berkovic, S.F., Scheffer, I.E., 2010. Absence epilepsies with widely variable onset are a key feature of familial GLUT1 deficiency. Neurology 75, 432–440.
Mullen, S.A., Marini, C., Suls, A., Mei, D., Della Giustina, E., Buti, D., Arsov, T., Damiano, J., Lawrence, K., De Jonghe, P., Berkovic, S.F., Scheffer, I.E., Guerrini, R., 2011. Glucose transporter 1 deficiency as a treatable cause of myoclonic astatic epilepsy. Arch. Neurol. 68 (9), 1152–1155.
Pascual, J.M., Van Heertum, R.L., Wang, D., Engelstad, K., De Vivo, D.C., 2002. Imaging the metabolic footprint of Glut1 deficiency on the brain. Ann. Neurol. 52, 458–464.
Pearson, T.S., Akman, C., Hinton, V.J., Engelstad, K., De Vivo, D.C., 2013. Phenotypic spectrum of glucose transporter type 1 deficiency syndrome (Glut1 DS). Curr. Neurol. Neurosci. Rep. 13, 342.
Pellerin, L., Magistretti, P.J., 2004. Neuroenergetics: calling upon astrocytes to satisfy hungry neurons. Neuroscientist 10, 53–62.
Pugnaghi, M., Carmichael, D.W., Vaudano, A.E., Chaudhary, U.J., Benuzzi, F., Di Bonaventura, C., Giallonardo, A.T., Rodionov, R., Walker, M.C., Duncan, J.S., Meletti, S., Lemieux, L., 2014. Generalized spike and waves: effect of discharge duration on brain networks as revealed by BOLD fMRI. Brain Topogr. 27, 123–137.
Ruggieri, A., Vaudano, A.E., Benuzzi, F., Serafini, M., Gessaroli, G., Farinelli, V., Nichelli, P.F., Meletti, S., 2015. Mapping (and modeling) physiological movements during EEG-fMRI recordings: the added value of the video acquired simultaneously. J. Neurosci. Methods 239, 223–237.
Seidner, G., Alvarez, M.G., Yeh, J.I., O'Driscoll, K.R., Klepper, J., Stump, T.S., Wang, D., Spinner, N.B., Birnbaum, M.J., De Vivo, D.C., 1998. GLUT-1 deficiency syndrome caused by haploinsufficiency of the blood-brain barrier hexose carrier. Nat. Genet. 18, 188–191.
Striano, P., Weber, Y.G., Toliat, M.R., Schubert, J., Leu, C., Chaimana, R., Baulac, S., Guerrero, R., LeGuern, E., Lehesjoki, A.E., Polvi, A., Robbiano, A., Serratosa, J.M., Guerrini, R., Nürnberg, P., Sander, T., Zara, F., Lerche, H., Marini, C., EPICURE Consortium, 2012. GLUT1 mutations are a rare cause of familial idiopathic generalized epilepsy. Neurology 78, 557–562.
Suls, A., Dedeken, P., Goffin, K., Van Esch, H., Dupont, P., Cassiman, D., Kempfle, J., Wuttke, T.V., Weber, Y., Lerche, H., Afawi, Z., Vandenberghe, W., Korczyn, A.D., Berkovic, S.F., Ekstein, D., Kivity, S., Ryvlin, P., Claes, L.R., Deprez, L., Maljevic, S., Vargas, A., Van Dyck, T., Goossens, D., Del-Favero, J., Van Laere, K., De Jonghe, P., Van Paesschen, W., 2008. Paroxysmal exercise-induced dyskinesia and epilepsy is due to mutations in SLC2A1, encoding the glucose transporter GLUT1. Brain 131, 1831–1844.
Suls, A., Mullen, S.A., Weber, Y.G., Verhaert, K., Ceulemans, B., Guerrini, R., Wuttke, T.V., Salvo-Vargas, A., Deprez, L., Claes, L.R., Jordanova, A., Berkovic, S.F., Lerche, H., De Jonghe, P., Scheffer, I.E., 2009. Early-onset absence epilepsy caused by mutations in the glucose transporter GLUT1. Ann. Neurol. 66, 415–419.
Vannucci, S.J., Maher, F., Simpson, I.A., 1997. Glucose transporter proteins in brain: delivery of glucose to neurons and glia. Glia 21 (1), 2–21.
Vaudano, A.E., Laufs, H., Kiebel, S.J., Carmichael, D.W., Hamandi, K., Guye, M., Thornton, R., Rodionov, R., Friston, K.J., Duncan, J.S., Lemieux, L., 2009. Causal hierarchy within the thalamo-cortical network in spike and wave discharges. PLoS One 4 (8), e6475.
Verrotti, A., D'Egidio, C., Agostinelli, S., Gobbi, G., 2012. Glut1 deficiency: when to suspect and how to diagnose? Eur. J. Paediatr. Neurol. 16 (1), 3–9.
Wang, D., Pascual, J.M., Yang, H., Engelstad, K., Jhung, S., Sun, R.P., De Vivo, D.C., 2005. Glut-1 deficiency syndrome: clinical, genetic, and therapeutic aspects. Ann. Neurol. 57, 111–118.
Zorzi, G., Castellotti, B., Zibordi, F., Gellera, C., Nardocci, N., 2008. Paroxysmal movement disorders in GLUT1 deficiency syndrome. Neurology 71, 146–148.